Progress In Electromagnetics Research, Vol. 155, 39–52, 2016

Fast Domain Decomposition Methods of FE-BI-MLFMA for 3D Scattering/Radiation Problems

Ming-Lin Yang, Hong-Wei Gao, Xu-Min Sun, and Xin-Qing Sheng*

(*Invited Paper*)

Abstract—It has been widely verified that the hybrid finite element - boundary integral - multilevel fast multipole algorithm (FE-BI-MLFMA) is a general, efficient and accurate method for the analysis of unbounded electromagnetic problems. A variety of fast methods of FE-BI-MLFMA have been developed since 1998. In particular, the domain decomposition methods have been applied to FE-BI-MLFMA and significantly improve the efficiency of FE-BI-MLFMA in recent years. A series of fast domain decomposition methods (DDMs) of FE-BI-MLFMA have been developed. These fast DDMs can be roughly classified into two types: Schwarz DDMs and dual-primal finite element tearing and interconnecting (FETI-DP) DDMs. This paper will first give an overview of the DDMs development of FE-BI-MLFMA. Then a uniform, consistent, and efficient formulation is presented and discussed for these fast DDMs of FE-BI-MLFMA. Their computational complexities are analyzed and studied numerically.

1. INTRODUCTION

The hybrid finite element - boundary integral - multilevel fast multipole algorithm (FE-BI-MLFMA) has been widely verified to be a powerful numerical technique for computing open region problems, such as scattering/radiation by objects with complex geometries and inhomogeneous media [1–13]. The method usually divides the solution domain into inhomogeneous interior and homogeneous exterior regions by the surface of an object. The field in the interior region is formulated by the finite element method (FEM), whereas the field in the exterior region is done by the boundary integral equation (BIE). Then the FE-BI matrix equation of the field in the total solution domain can be established by the field continuity conditions at the boundary surface. The final FE-BI matrix equation is solved by iterative solvers, where the key step of matrix-vector multiplication in iterative solvers is accelerated by MLFMA.

Since FE-BI-MLFMA was successfully developed in 1998 [1], a series of works have been made to further improve the efficiency of FE-BI-MLFMA. These works can be categorized into two groups. One is to employ higher-order basis functions to reduce the number of unknowns [5–8]; the other is to employ preconditioners to speed up the convergence of iterative solvers [9–13]. Since the condition number of the FEM matrix is usually large, the FE-BI matrix is not well-conditioned, sometimes even becomes ill-conditioned for large and complex objects. Hence, the problem of slow convergence or non-convergence becomes the bottleneck of FE-BI-MLFMA. Although many preconditioners have been proposed to speed up the convergence of FE-BI-MLFMA in [5–8], they are not satisfied until the domain decomposition methods are applied to FE-BI-MLFMA. Because the construction of these preconditioners essentially requires the inverse of the FEM matrix, the cost of constructing preconditioners for the FE-BI matrix

Received 28 October 2015, Accepted 9 February 2016, Scheduled 23 February 2016
Invited paper for the Commemorative Collection on the 150-Year Anniversary of Maxwell's Equations.
* Corresponding author: Xin-Qing Sheng (xsheng@bit.edu.cn).
The authors are with the Center for Electromagnetic Simulation, School of Information and Electronics, Beijing Institute of Technology, Beijing 100081, China.

equation is expensive. The application of domain decomposition methods (DDMs) fundamentally reduces the computational complexity of solution to FEM matrix equations.

There are various types of domain decomposition methods [14–17]. Over the past one decade, many domain decomposition methods have been developed in computational electromagnetics [18–24]. These domain decomposition methods can be roughly categorized into two types. One is the Schwarz domain decomposition method (SDDM). This SDDM first requires the inverse of the FEM matrix in each subdomain, and then performs the iterative solution of the global interface problems established with the Robin transmission condition (RTC). The other type is the dual-primal finite element tearing and interconnecting (FETI-DP). FETI-DP first divides the whole solution domain into many subdomains. These subdomains are separated at the interface between subdomains by the introduced Lagrange Multiplier (LM) or the cement-elements (CE), but connected at the corners shared by many (more than two) subdomains. The field in each subdomain is solved and represented by the interface unknowns. Finally, the matrix equation corresponding to the interface unknowns is solved by iterative solvers [24]. In recent years, these domain decomposition methods have been applied to FE-BI-MLFMA, and many fast domain decomposition methods have been developed. The SDDM of FE-BI has been developed in [25, 26]. The conformal FETI-DP DDM of FE-BI-MLFMA has been developed in [27–29] by using FETI-DP DDM. Based on these studies in [25–29], this paper will present a uniform, consistent, efficient formulation of FE-BI-MLFMA for conformal/non-conformal Schwarz algorithm, and conformal/non-conformal FETI-DP. The computational complexities of these fast DDMs are analyzed and studied numerically.

The rest of the paper is organized as follows. The uniform formulation for fast domain decomposition algorithms of FE-BI-MLFMA is presented in Section 2. Section 3 studies the computational complexity of the presented DDM of FE-BI-MLFMA numerically. Conclusions are given in Section 4.

2. FORMULATION FOR FAST DDMS OF FE-BI-MLFMA

Consider the scattering by an arbitrarily shaped inhomogeneous body. In FE-BI-MLFMA, the solution region is usually divided into the interior and the exterior regions by the surface of the inhomogeneous object, denoted here as S [1]. The interior region V is further divided into many subdomains, as shown in Fig. 1. Suppose the meshes of the surface S in the interior and exterior regions are non-conformal, $\Gamma_{n,S}$ denotes the interior surface in the nth subdomain, and $\Gamma_{S,n}$ denotes the exterior surface. The field in subdomain V_m is formulated into an equivalent variational problem with the functional given by:

$$\begin{aligned} F(\mathbf{E}_m) \;=\; & \frac{1}{2}\iiint_{V_m}\left[(\nabla\times \mathrm{E}_m)\cdot\left(\mu_{m,r}^{-1}\nabla\times \mathrm{E}_m\right)-k_0^2\varepsilon_{m,r}\mathrm{E}_m\cdot \mathrm{E}_m\right]dV \\ & -jk_0Z_0\iiint_{V_m}\mathrm{E}_m\cdot\mathbf{J}_m dV+jk_0\iint_{\Gamma_m}\left(\mathrm{E}_m\times\bar{\mathbf{H}}_m\right)\cdot\hat{n}_m d\Gamma \end{aligned} \tag{1}$$

where $\bar{\mathbf{H}}_m = Z_0\mathbf{H}_m$, Z_0 is the intrinsic impedance in the free-space, k_0 the free-space wave number, and $\hat{n}_m$ the outward unit vector normal to Γ_m. The field in the exterior region is usually formulated into the following combined field integral equation (CFIE) [1]

$$\begin{aligned} & \pi_t\left(-\frac{1}{2}\mathbf{E}_S+\mathbf{L}\left(\hat{n}\times\bar{\mathbf{H}}_S\right)-\mathbf{K}\left(\mathbf{E}_S\times\hat{n}\right)\right)+\pi_\times\left(\left[-\frac{1}{2}\bar{\mathbf{H}}_S+\mathbf{L}\left(\mathbf{E}_S\times\hat{n}\right)+\mathbf{K}\left(\hat{n}\times\bar{\mathbf{H}}_S\right)\right]\right) \\ & = -\pi_t\left(\mathbf{E}^i\right)-\pi_\times\left(\bar{\mathbf{H}}^i\right) \end{aligned} \tag{2}$$

where $\pi_t(\cdot)\hat{n}\times(\cdot)\times\hat{n}$ is the surface tangential operator; $\pi_\times(\cdot)\hat{n}\times(\cdot)$ is the surface twist tangential operator; $\mathbf{E}^i$ and $\bar{\mathbf{H}}^i$ are the impressed electromagnetic fields; $\mathbf{L}$ and $\mathbf{K}$ are the integral-differential operators defined by

$$\mathbf{L}(\mathbf{X}) \;=\; -jk_0\int_S\left[\mathbf{I}+\frac{1}{k_0^2}\nabla\nabla'\cdot\right]\mathbf{X}(\mathbf{r}')G_0(\mathbf{r},\mathbf{r}')dS \tag{3}$$

$$\mathbf{K}(\mathbf{X}) \;=\; \int_S\nabla G_0\left(\mathbf{r},\mathbf{r}'\right)\times\mathbf{X}(\mathbf{r}')dS \tag{4}$$

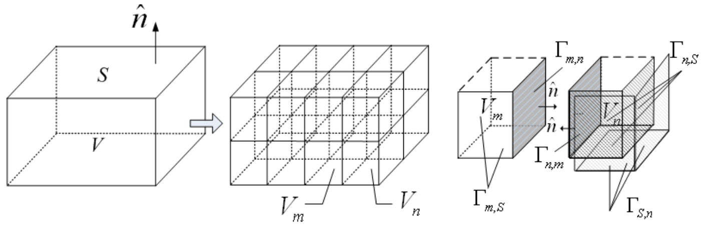

Figure 1. Illustration of domain decomposition method of FE-BI-MLFMA.

where $\mathbf{I}$ is the identity matrix. The singular point $\mathbf{r} = \mathbf{r}'$ is removed in Eq. (4).

To apply DDMs to FE-BI-MLFMA, we need to consider how to connect the field between interior subdomains, and between interior and exterior regions. There are two kinds of boundary conditions to connect subdomains, namely the *Robin-type transmission condition* (RTC) and the *Dirichlet transmission condition* (DTC). The RTC can be enforced by two approaches: one is called as the Lagrange Multiplier-based (LM), the other is called as the cement-element based (CE) [24]. Our recent study shows that RTC is better than DTC to connect interior subdomains, whereas DTC is better than RTC to connect interior and exterior regions. The reasons are as follows: (1) the FEM matrix for each interior subdomain is equivalent to an open system and is immune to the resonant problem when RTC is used at the interface. In contrast, when DTC is used, the FEM matrix for each interior subdomain is equivalent to a close system and suffers from the resonant problem; (2) when considering the connection between the interior FEM and exterior BI regions, the BI itself can be considered as an infinite higher order RTC to connect the FEM and BI region. Furthermore, because the electromagnetic field used in the CE approach is more compatible with the field in BI than the Lagrange multipliers used in the LM approach, the CE approach is better than the LM approach to implement RTC for the FE-BI system, especially for nonconformal cases. Hence, we employ the following RTC to connect the field between interior subdomains

$$\alpha\pi_t\left(\mathbf{E}_m\right) + jk_0\pi_\times\left(\bar{\mathbf{H}}_m\right) = \alpha\pi_t\left(\mathbf{E}_n\right) - jk_0\pi_\times\left(\bar{\mathbf{H}}_n\right), \tag{5}$$

and employ the following DTC to connect field between interior and exterior regions

$$\begin{cases} \pi_t\left(\mathbf{E}_m\right) = \pi_t\left(\mathbf{E}_S\right) \\ \pi_\times\left(\bar{\mathbf{H}}_m\right) = -\pi_\times\left(\bar{\mathbf{H}}_S\right) \end{cases} \tag{6}$$

In Eq. (5), the parameter α is complex, usually chosen as jk_0 to make the DDM system well posed. Hence throughout the paper, we let $\alpha = jk_0$. By making use of the connection conditions of Eqs. (5) and (6), a uniform formulation of various DDMs of FE-BI-MLFMA can be presented as follows.

2.1. Conformal Schwarz DDM

Equations (1) and (5) in the mth subdomain can be discretized by using the conventional FEM as

$$\begin{bmatrix} K_m & B_{m,bb} \\ (B_{m,bb})^T & C_{m,bb} \end{bmatrix} \begin{Bmatrix} E_m \\ \bar{H}_{m,b} \end{Bmatrix} = \begin{Bmatrix} f_m - B_{m,sS}\bar{H}_S \\ g_{m,b} \end{Bmatrix} \tag{7}$$

where the subscript 'b' stands for the interface of the mth subdomain with other subdomains, but does not include that with the boundary surface of S. The second term of the first line in the right hand side of Eq. (7) does not exist if the mth subdomain does not connect with the boundary surface of S, and

$$[K_m] = \iiint_{V_m} \left[\left(\mu_{m,r}^{-1}(\nabla\times\{\mathbf{N}_m\})\cdot(\nabla\times\{\mathbf{N}_m\})^T - k_0^2\varepsilon_{m,r}\{\mathbf{N}_m\}\cdot\{\mathbf{N}_m\}^T\right)\right] dV \tag{8}$$

$$[B_{m,bb}] = -jk_0\iint_{\Gamma_{m,b}} \{\mathbf{N}_{m,b}\}\cdot\{\mathbf{N}_{m,b}\}^T dS, \quad [B_{m,sS}] = jk_0\iint_{\Gamma_{m,s}} \{\mathbf{N}_S\}\cdot\{\hat{n}\times\mathbf{N}_S\}^T dS \tag{9}$$

$$[C_{m,bb}] = -jk_0\iint_{\Gamma_{m,b}} \{\mathbf{N}_{m,b}\}\cdot\{\mathbf{N}_{m,b}\}^T dS \tag{10}$$

$$\{g_{m,b}\} = \sum_{n\in\text{neighbor}(m)} [U_{m,mn}\ V_{m,mn}]\{u_{n,b}\} = \sum_{n\in\text{neighbor}(m)} [T_{m,n}]\{u_{n,b}\}, \tag{11}$$

with

$$\{u_{n,b}\} = \left\{ \begin{array}{c} E_{n,b} \\ \bar{H}_{n,b} \end{array} \right\}, \quad [U_{m,mn}] = -jk_0 \iint_{\Gamma_{m,n}} \{\mathbf{N}_{m,b}\} \cdot \{\mathbf{N}_{n,b}\}^T dS,$$
$$[V_{m,mn}] = jk_0 \iint_{\Gamma_{m,n}} \{\mathbf{N}_{m,b}\} \cdot \{\mathbf{N}_{n,b}\}^T dS \tag{12}$$

where $\mathbf{N}_m$, $\mathbf{N}_S$, $\mathbf{N}_b$ are the vector basis functions respectively defined in the interior volume element, boundary surface element, and interface surface element. $\{g_{m,b}\}$ denotes the contribution from the interface unknowns of all neighbors of the mth subdomain. In SDDM, the unknowns in each subdomain are grouped into the interior and interface unknowns. Thus Eq. (7) can be rewritten as

$$\left[\begin{array}{ccc} K_{m,ii} & K_{m,ib} & 0 \\ K_{m,bi} & K_{m,bb} & B_{m,bb} \\ & (B_{m,bb})^T & C_{m,bb} \end{array} \right] \left\{ \begin{array}{c} E_{m,i} \\ E_{m,b} \\ \bar{H}_{m,b} \end{array} \right\} = \left\{ \begin{array}{c} f_{m,i} - B_{m,sS}\bar{H}_S \\ f_{m,b} \\ g_{m,b} \end{array} \right\} \tag{13}$$

For the sake of clarity, let

$$\{u_m\} = \left\{ \begin{array}{c} u_{m,i} \\ u_{m,b} \end{array} \right\} = \left\{ \begin{array}{c} E_{m,i} \\ E_{m,b} \\ \bar{H}_{m,b} \end{array} \right\}, \quad [A_m] = \left[\begin{array}{ccc} K_{m,ii} & K_{m,ib} & 0 \\ K_{m,bi} & K_{m,bb} & B_{m,bb} \\ & (B_{m,bb})^T & C_{m,bb} \end{array} \right], \tag{14}$$

and the projection Boolean matrices $[R_{m,i}]$, $[R_{m,b}]$, $[R_{m,Eb}]$ and $[R_{m,Hb}]$ satisfy $\{u_{m,i}\} = [R_{m,i}]\{u_m\}$, $\{u_{m,b}\} = [R_{m,b}]\{u_m\}$, $\{E_{m,b}\} = [R_{m,Eb}]\{u_{m,b}\}$, $\{\bar{H}_{m,b}\} = [R_{m,Hb}]\{u_{m,b}\}$. Then, $\{u_m\}$ can be represented as

$$\begin{aligned} \{u_m\} = [A_m]^{-1} \Big(& [R_{m,i}]^T \left\{ f_{m,i} - B_{m,sS}\bar{H}_S \right\} + [R_{m,b}]^T [R_{m,Eb}]^T \{f_{m,b}\} \\ & + [R_{m,b}]^T [R_{m,Hb}]^T \sum_{n \in \text{neighbor}(m)} [T_{m,n}] \{u_{n,b}\} \Big) \end{aligned} \tag{15}$$

Thus, the interface equation only related to the unknowns at interfaces can be obtained as

$$\begin{aligned} \{u_{m,b}\} = [R_{m,b}] [A_m]^{-1} \Big(& [R_{m,i}]^T \left\{ f_{m,i} - B_{m,sS}\bar{H}_S \right\} + [R_{m,b}]^T [R_{m,Eb}]^T \{f_{m,b}\} \\ & + [R_{m,b}]^T [R_{m,Hb}]^T \sum_{n \in \text{neighbor}(m)} [T_{m,n}] \{u_{n,b}\} \Big) \end{aligned} \tag{16}$$

The other equation related to the unknowns inside each subdomain can be represented as

$$\begin{aligned} \{u_{m,i}\} = [R_{m,i}] [A_m]^{-1} \Big(& [R_{m,i}]^T \left\{ f_{m,i} - B_{m,sS}\bar{H}_S \right\} + [R_{m,b}]^T [R_{m,Eb}]^T \{f_{m,b}\} \\ & + [R_{m,b}]^T [R_{m,Hb}]^T \sum_{n \in \text{neighbor}(m)} [T_{m,n}] \{u_{n,b}\} \Big) \end{aligned} \tag{17}$$

Assembling Eq. (16) in all subdomains yields

$$[\tilde{K}_{bb}]\{u_b\} + [\tilde{K}_{bS}]\{\bar{H}_S\} = \{\tilde{f}_b\} \tag{18}$$

where

$$[\tilde{K}_{bb}] = [I] - \sum_{m=1}^{N_s} \left([R_{mb}]^T [R_{m,b}] [A_m]^{-1} [R_{m,b}]^T [R_{m,Hb}]^T \sum_{n \in \text{neighbor}(m)} [T_{m,n}] [R_{nb}] \right)$$
$$[\tilde{K}_{bS}] = \sum_{m=1}^{N_s} [R_{m,Hb}]^T [R_{m,b}] [A_m]^{-1} [R_{m,i}]^T [B_{m,sS}] \tag{19}$$
$$\{\tilde{f}_b\} = \sum_{m=1}^{N_s} [R_{mb}]^T [R_{m,b}] [A_m]^{-1} \left([R_{m,i}]^T \{f_{m,i}\} + [R_{m,b}]^T [R_{m,Eb}]^T \{f_{m,b}\} \right)$$

The Boolean matrix of $[R_{mb}]$ satisfies $\{u_{m,b}\} = [R_{mb}]\{u_b\}$.

Equation (2) for the field in the exterior region can also be discretized by the method of moment (MoM) with the Rao-Wilton-Glisson (RWG) basis function [30] as

$$[P]\{E_S\} + [Q]\{\bar{H}_S\} = \{f_S\} \tag{20}$$

where

$$P_{mn} = \frac{1}{2}\int_S \mathbf{g}_m \cdot (\hat{n} \times \mathbf{g}_n)dS - \int_S \mathbf{g}_m \cdot \mathbf{K}(\mathbf{g}_n)\, dS + \int_S (\hat{n} \times \mathbf{g}_m) \cdot \mathbf{L}(\mathbf{g}_n)\, dS \tag{21}$$

$$Q_{mn} = -\frac{1}{2}\int_S (\hat{n} \times \mathbf{g}_m) \cdot (\hat{n} \times \mathbf{g}_n)dS + \int_S \mathbf{g}_m \cdot \mathbf{L}(\mathbf{g}_n)\, dS + \int_S (\hat{n} \times \mathbf{g}_m) \cdot \mathbf{K}(\mathbf{g}_n)\, dS \tag{22}$$

$$f_m = \int_S \mathbf{g}_m \cdot \mathbf{E}^i(\mathbf{r})\, dS + \int_S (\hat{n} \times \mathbf{g}_m) \cdot \mathbf{H}^i(\mathbf{r})\, dS \tag{23}$$

According to Eq. (6), we have

$$\begin{aligned}\{E_S\} &= \{E_F\} = \sum_{m=1}^{N_s} E_{m,s} = \sum_{m=1}^{N_s} [R_{m,si}]\{u_{m,i}\} \\ &= \sum_{m=1}^{N_s} [R_{m,si}][R_{m,i}]\,[A_m]^{-1}\Bigg([R_{m,i}]^T\left\{f_{m,i} - B_{m,sS}\bar{H}_S\right\} + [R_{m,b}]^T[R_{m,Eb}]^T\left\{f_{m,b}\right\} \\ &\quad + [R_{m,b}]^T[R_{m,Hb}]^T \sum_{n\in\,\text{neighbor}(m)} [T_{m,n}]\left\{u_{n,b}\right\}\Bigg)\end{aligned} \tag{24}$$

Substituting Eq. (24) into Eq. (20), we can obtain another matrix equation as

$$[\tilde{K}_{Sb}]\{u_b\} + [\tilde{K}_{SS}]\{\bar{H}_S\} = \{\tilde{f}_S\} \tag{25}$$

where

$$[\tilde{K}_{Sb}] = [P] \sum_{m\in\,\text{neighbor}(S)} \left([R_{m,si}][R_{m,i}]\,[A_m]^{-1}\,[R_{m,b}]^T[R_{m,Hb}]^T \sum_{n\in\,\text{neighbor}(m)} [T_{m,n}]\,[R_{nb}]\right) \tag{26}$$

$$[\tilde{K}_{SS}] = [Q] - [P] \sum_{m\in\,\text{neighbor}(S)} \Big([R_{m,si}][R_{m,i}]\,[A_m]^{-1}\,[R_{m,i}]^T[B_{m,sS}]\Big) \tag{27}$$

$$\{\tilde{f}_S\} = \{f_s\} - [P] \sum_{m\in\,\text{neighbor}(S)} [R_{m,si}][R_{m,i}]\,[A_m]^{-1}\left([R_{m,i}]^T\left\{f_{m,i}\right\} + [R_{m,b}]^T[R_{m,Eb}]^T\left\{f_{m,b}\right\}\right) \tag{28}$$

Equations (18) and (25) form the final matrix equation system. Hence, the original volume problem is reduced to the surface problem only for the unknowns at the interfaces. It can be efficiently solved by using iterative solvers such as GMRES with the aid of MLFMA which significantly speeds up the matrix-vector multiplication of $[P]\{E_S\}$ and $[Q]\{\bar{H}_S\}$.

2.2. Non-Conformal Schwarz DDM

When the mesh is non-conformal, the final matrix equation system can be obtained in a similar way as described in Section 2.1. The difference of implementation between conformal and non-conformal cases only exists at the interfaces between subdomains. For the interface between interior subdomains, the implementation of non-conformal cases is essentially the same as that of conformal cases since RTC is employed here and the unknowns at the interface for each subdomain are different and independent. It is worth to point out that the integrals in Eqs. (9) and (12) should be more carefully evaluated due to non-conformal meshes. For the interface between FEM and BI, the following special treatments are required since DTC is employed here.

Since the meshes between FEM and BI are non-conformal, there is no direct explicit relation of the electric field at the boundary surface between the FEM and BI domains. To find their relation, we impose the Dirichlet transmission condition of Eq. (6) in a weak form. To be more specific, Eq. (6) is discretized as

$$[M_{SS}]\{E_S\} = [N_{SF}]\{E_F\} \tag{29}$$

with

$$[M_{SS}] = \iint_S \{\hat{n}_S \times \mathbf{N}_S\} \cdot \{\hat{n}_S \times \mathbf{N}_S\}^T dS \tag{30}$$

$$[N_{SF}] = \iint_S \{\hat{n}_S \times \mathbf{N}_S\} \cdot \{\hat{n}_S \times \mathbf{N}_F\}^T dS \tag{31}$$

where $\mathbf{N}_F$ and $\mathbf{N}_S$ are vector basis functions defined in the meshes of the interior subdomain surface and boundary surface respectively. Hence, the electric field at the boundary surface can be explicitly expressed by the electric field at the interior subdomain surface as

$$\{E_S\} = \left[T^{SF}\right]\{E_F\} \tag{32}$$

where $[T^{SF}] = [M_{SS}]^{-1}[N_{SF}]$. Substituting Eq. (32) into Eq. (20) yields

$$[P]\left[T^{SF}\right]\{E_F\} + [Q]\left\{\bar{H}_S\right\} = \{f_S\} \tag{33}$$

Then for non-conformal cases, Eqs. (26)–(28) are changed to be

$$[\tilde{K}_{Sb}] = [P][T^{SF}] \sum_{m\in \text{neighbor}(S)} \left([R_{m,si}][R_{m,i}]\,[A_m]^{-1}\,[R_{m,b}]^T [R_{m,Hb}]^T \sum_{n\in \text{neighbor}(m)} [T_{m,n}]\,[R_{nb}] \right) \tag{34}$$

$$[\tilde{K}_{SS}] = [Q] - [P][T^{SF}] \sum_{m\in \text{neighbor}(S)} \left([R_{m,si}][R_{m,i}]\,[A_m]^{-1}\,[R_{m,i}]^T [B_{m,sS}] \right) \tag{35}$$

$$\{\tilde{f}_S\} = \{f_s\} - [P][T^{SF}] \sum_{m\in \text{neighbor}(S)} [R_{m,si}][R_{m,i}][A_m]^{-1} \left([R_{m,i}]^T\{f_{m,i}\} + [R_{m,b}]^T [R_{m,Eb}]^T\{f_{m,b}\} \right) \tag{36}$$

2.3. Conformal FETI-DP DDM

The essential difference of FETI-DP DDM from SDDM is that there is a special 'global' corner preconditioner, which makes the final matrix equation system better conditioned. In FETI-DP DDM, the unknowns in the mth subdomain are grouped into three categories: interior unknowns, interface unknowns at the interface, and corner unknowns at the edges shared by more than two subdomains, noted as $\{\mathbf{E}_{m,i}\}$, $\{\mathbf{E}_{m,b}\}$, $\{\mathbf{E}_{m,c}\}$ respectively. Thus Eq. (7) can be written as

$$\begin{bmatrix} K_{m,ii} & K_{m,ib} & K_{m,ic} & 0 \\ K_{m,bi} & K_{m,bb} & K_{m,bc} & B_{m,bb} \\ K_{m,ci} & K_{m,cb} & K_{m,cc} & 0 \\ 0 & (B_{m,bb})^T & 0 & C_{m,bb} \end{bmatrix} \begin{Bmatrix} E_{m,i} \\ E_{m,b} \\ E_{m,c} \\ \bar{H}_{m,b} \end{Bmatrix} = \begin{Bmatrix} f_{m,i} - B_{m,iS}\bar{H}_S \\ f_{m,b} \\ f_{m,c} - B_{m,cS}\bar{H}_S \\ g_{m,b} \end{Bmatrix} \tag{37}$$

where $[B_{m,iS}]$ and $[B_{m,cS}]$ are the submatrices of $[B_{m,sS}]$. After re-ordering the unknowns in each subdomain, we obtain

$$\begin{bmatrix} K_{m,ii} & K_{m,ib} & 0 & K_{m,ic} \\ K_{m,bi} & K_{m,bb} & B_{m,bb} & K_{m,bc} \\ 0 & (B_{m,bb})^T & C_{m,bb} & 0 \\ K_{m,ci} & K_{m,cb} & 0 & K_{m,cc} \end{bmatrix} \begin{Bmatrix} E_{m,i} \\ E_{m,b} \\ \bar{H}_{m,b} \\ E_{m,c} \end{Bmatrix} = \begin{Bmatrix} f_{m,i} - B_{m,iS}\bar{H}_S \\ f_{m,b} \\ g_{m,b} \\ f_{m,c} - B_{m,cS}\bar{H}_S \end{Bmatrix} \tag{38}$$

which can be further written in a compact form as

$$\begin{bmatrix} K_{m,rr} & K_{m,rc} \\ K_{m,cr} & K_{m,cc} \end{bmatrix} \begin{Bmatrix} u_{m,r} \\ E_{m,c} \end{Bmatrix} = \begin{Bmatrix} f_{m,r} + (R_{m,br})^T (R_{m,Hb})^T g_{m,b} - (R_{m,ir})^T B_{m,iS}\bar{H}_S \\ f_{m,c} - B_{m,cS}\bar{H}_S \end{Bmatrix} \tag{39}$$

with

$$[K_{m,rr}] = \begin{bmatrix} K_{m,ii} & K_{m,ib} & 0 \\ K_{m,bi} & K_{m,bb} & B_{m,bb} \\ 0 & (B_{m,bb})^T & C_{m,bb} \end{bmatrix}, \quad [K_{m,rc}] = \begin{bmatrix} K_{m,ic} \\ K_{m,bc} \\ 0 \end{bmatrix}$$
$$[K_{m,cr}] = \begin{bmatrix} K_{m,ci} & K_{m,cb} & 0 \end{bmatrix}, \quad \{u_{m,r}\} = \left\{ \begin{array}{c} u_{m,i} \\ u_{m,b} \end{array} \right\} = \left\{ \begin{array}{c} E_{m,i} \\ E_{m,b} \\ \bar{H}_{m,b} \end{array} \right\}, \quad \{f_{m,r}\} = \left\{ \begin{array}{c} f_{m,i} \\ f_{m,b} \\ 0 \end{array} \right\} \tag{40}$$

where $[R_{m,ir}]$, $[R_{m,br}]$, $[R_{m,Eb}]$ and $[R_{m,Hb}]$ are Boolean matrices. The latter two are the same as before, the first two satisfy

$$\{E_{m,i}\} = [R_{m,ir}]\{u_{m,r}\}, \quad \{u_{m,b}\} = [R_{m,br}]\{u_{m,r}\} \tag{41}$$

From Eq. (39), we have

$$\{u_{m,r}\} = [K_{m,rr}]^{-1} \left(\{f_{m,r}\} + [R_{m,br}]^T [R_{m,Hb}]^T \{g_{m,b}\} - [R_{m,ir}]^T [B_{m,iS}]\{\bar{H}_S\} - [K_{m,rc}]\{E_{m,c}\}\right) \tag{42}$$

$$\left([K_{m,cc}] - [K_{m,cr}][K_{m,rr}]^{-1}[K_{m,rc}]\right)\{E_{m,c}\} = \{f_{m,c}\} - [B_{m,cS}]\{\bar{H}_S\} - [K_{m,cr}][K_{m,rr}]^{-1}\{f_{m,r}\}$$
$$-[K_{m,cr}][K_{m,rr}]^{-1}\left([R_{m,br}]^T [R_{m,Hb}]^T g_{m,b} - [R_{m,ir}]^T [B_{m,iS}]\{\bar{H}_S\}\right) \tag{43}$$

Assembling Eq. (43) in all interior subdomains and using Eq. (11) yield the following global equation for the primal corner unknowns $\{E_c\}$ as

$$[\tilde{K}_{cc}]\{E_c\} = \{\tilde{f}_c\} + [\tilde{K}_{cb}]\{u_b\} + [\tilde{K}_{cS}]\{\bar{H}_S\} \tag{44}$$

where

$$[\tilde{K}_{cc}] = \sum_{m=1}^{N_s} [R_{mc}]^T \left([K_{m,cc}] - [K_{m,cr}][K_{m,rr}]^{-1}[K_{m,rc}]\right)[R_{mc}] \tag{45}$$

$$[\tilde{K}_{cb}] = -\sum_{m=1}^{N_s} (R_{mc})^T \left([K_{m,cr}][K_{m,rr}]^{-1}[R_{m,br}]^T [R_{m,Hb}]^T \sum_{n \in \text{neighbor}(m)} \left([U_{m,mn} \quad V_{m,mn}][R_{nb}]\right)\right) \tag{46}$$

$$[\tilde{K}_{cS}] = \sum_{m=1}^{N_s} [R_{mc}]^T \left([K_{m,cr}][K_{m,rr}]^{-1}[R_{m,ir}]^T [B_{m,iS}] - [B_{m,cS}]\right) \tag{47}$$

$$[\tilde{f}_c] = \sum_{m=1}^{N_s} (R_{mc})^T \left(\{f_{m,c}\} - [K_{m,cr}][K_{m,rr}]^{-1}\{f_{m,r}\}\right) \tag{48}$$

where $[R_{mc}]$ is the projection Boolean matrix which satisfies $\{E_{m,c}\} = [R_{mc}]\{E_c\}$, $\{u_b\}$ is the electric and magnetic field unknown coefficients at the interfaces of all subdomains and $[R_{nb}]$ is a Boolean projection matrix extracting $\{u_{n,b}\}$ from $\{u_b\}$. Thus $\{E_c\}$ can be formulated with $\{u_b\}$ and $\{\bar{H}_S\}$ as:

$$\{E_c\} = [\tilde{K}_{cc}]^{-1}\left(\{\tilde{f}_c\} + [\tilde{K}_{cb}]\{u_b\} + [\tilde{K}_{cS}]\{\bar{H}_S\}\right) \tag{49}$$

From Eq. (42), we can obtain the electric and magnetic field unknown coefficients $\{u_{m,b}\}$ at the interfaces of the mth subdomain as

$$\{u_{m,b}\} = [R_{m,br}]\{u_{m,r}\} = [R_{m,br}][K_{m,rr}]^{-1}\Big[\{f_{m,r}\} + [R_{m,br}]^T [R_{m,Hb}]^T \{g_m\}$$
$$-[R_{m,ir}]^T [B_{m,iS}]\{\bar{H}_S\} - [K_{m,rc}]\{E_{m,c}\}\Big] \tag{50}$$

Assembling Eq. (50) in all interior subdomains with the aid of Eq. (11) yields

$$[\tilde{K}_{bb}]\{u_b\} + [\tilde{K}_{bS}]\{\bar{H}_S\} + [\tilde{K}_{bc}]\{E_c\} = \{\tilde{f}_b\} \tag{51}$$

where

$$
\begin{aligned}
[\tilde{K}_{bb}] &= [I]-\sum_{m=1}^{N_s}\left([R_{mb}]^T[R_{m,br}][K_{m,rr}]^{-1}[R_{m,br}]^T\,[R_{m,Hb}]^T\sum_{n\in\,\text{neighbor}(m)}([U_{m,mn}\;\;V_{m,mn}][R_{nb}])\right)\\
[\tilde{K}_{bS}] &= \sum_{m=1}^{N_s}[R_{mb}]^T[R_{m,br}][K_{m,rr}]^{-1}[R_{m,ir}]^T[B_{m,iS}]\\
[\tilde{K}_{bc}] &= \sum_{m=1}^{N_s}[R_{mb}]^T[R_{m,br}][K_{m,rr}]^{-1}[K_{m,rc}][R_{mc}]\\
\{\tilde{f}_b\} &= \sum_{m=1}^{N_s}[R_{mb}]^T[R_{m,br}][K_{m,rr}]^{-1}\{f_{m,r}\}
\end{aligned}
\tag{52}
$$

According to Eq. (42), we have

$$
\begin{aligned}
\{E_S\} &= \{E_F\}=\sum_{m=1}^{N_s}E_{m,s}=\sum_{m=1}^{N_s}([R_{m,sr}]\{u_{m,r}\}+\{E_{m,c}\})\\
&= \sum_{m=1}^{N_s}\Bigg([R_{m,sr}][K_{m,rr}]^{-1}\Big[\{f_{m,r}\}+[R_{m,br}]^T\,[R_{m,Hb}]^T\,\{g_{m,b}\}\\
&\qquad -[R_{m,ir}]^T[B_{m,iS}]\{\bar{H}_S\}-[K_{m,rc}]\{E_{m,c}\}\Big]+\{E_{m,c}\}\Bigg)
\end{aligned}
\tag{53}
$$

By substituting Eq. (53) into Eq. (20), then using Eq. (11), we have

$$
[\tilde{K}_{Sb}]\{u_b\}+[\tilde{K}_{SS}]\{\bar{H}_S\}+[\tilde{K}_{Sc}]\{E_c\}=\{\tilde{f}_S\}
\tag{54}
$$

where

$$
[\tilde{K}_{Sb}]=[P]\sum_{m\in\,\text{neighbor}(S)}\left([R_{m,sr}][K_{m,rr}]^{-1}[R_{m,rb}]^T[R_{m,Hb}]^T\sum_{n\in\text{neighbor}(m)}([U_{m,mn}\;\;V_{m,mn}][R_{nb}])\right)
\tag{55}
$$

$$
[\tilde{K}_{SS}]=[Q]-[P]\sum_{m\in\,\text{neighbor}(S)}\big([R_{m,sr}][K_{m,rr}]^{-1}[R_{m,ir}]^T[B_{m,iS}]\big)
\tag{56}
$$

$$
[\tilde{K}_{Sc}]=[P]\sum_{m\in\,\text{neighbor}(S)}\big(-[R_{m,sr}][K_{m,rr}]^{-1}[K_{m,rc}]+I\big)\,[R_{mc}]
\tag{57}
$$

$$
\{\tilde{f}_S\}=\{f_s\}-[P]\sum_{m\in\,\text{neighbor}(S)}[R_{m,sr}]^T[K_{m,rr}]^{-1}\{f_{m,r}\}
\tag{58}
$$

Substituting Eq. (49) into Eqs. (51) and (54), the final matrix equation system only related to unknowns $\{u_b\}$ and $\{\bar{H}_S\}$ can be obtained. The inverse of $[\tilde{K}_{cc}]$ in Eq. (49) used by Eqs. (51) and (54), referred to as the coarse problem [19], is global, which needs to be solved first. This coarse problem couples all the subdomains by propagating the error globally at each iteration and increases the convergence rate [19].

2.4. Non-Conformal FETI-DP DDM

When the mesh is non-conformal, the final matrix equation system can be obtained in a similar way as described in Subsection 2.3. Besides special treatments for the unknowns at the FE-BI interface described in Subsection 2.2, another treatment related to the 'corner' unknowns is also required.

According to the FETI-DP DDM, a preconditioner matrix related to global primal variables $\{E_c\}$ is constructed by assembling Eq. (49) in all interior subdomains to speed up the convergence of the iterative solution of the interface equation. It is difficult for non-conformal meshes because the number

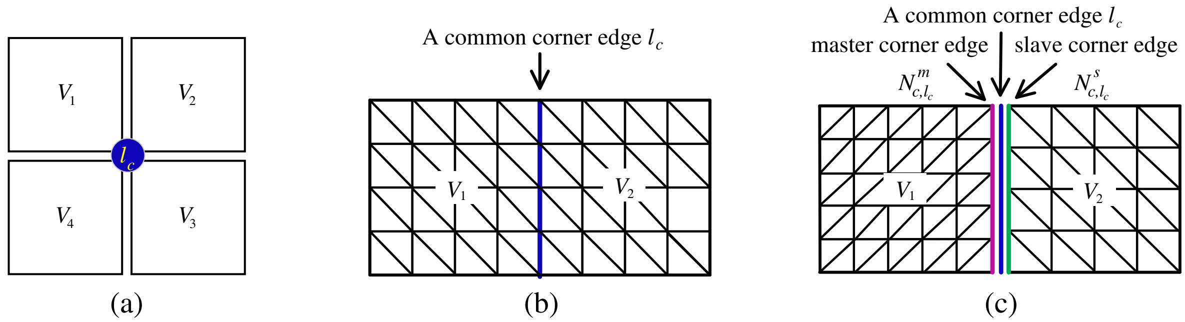

Figure 2. Conformal and non-conformal mesh case for a common corner edge.

of unknowns at a common corner edge for different shared subdomains is usually different as shown in Fig. 2. Fig. 2(a) shows the four subdomains sharing a common corner edge of l_c. Figs. 2(b) and 2(c) show the meshes of the interface between subdomains V_1 and V_2 sharing l_c for conformal and non-conformal cases respectively.

To deal with the aforementioned problem, the local corner edges from the shared subdomains for a common corner edge are grouped into one "master" local corner edge and other "slave" local corner edges as Fig. 2(c) [23]. The "master" local corner edge has the largest number of unknowns compared with the "slave" local corner edges. The unknowns from all "master" local corners are regarded as $\{E_c\}$. We impose the Dirichlet continuity condition $\mathbf{E}_t^m = \mathbf{E}_t^s$ at l_c, expand $\mathbf{E}_t^m$, $\mathbf{E}_t^s$ by vector basis functions $\{\mathbf{N}_{c,l_c}^m\}$, $\{\mathbf{N}_{c,l_c}^s\}$ and test both sides using $\{\mathbf{N}_{c,l_c}^s\}$, then the slave vector of $\{E_{c,l_c}^s\}$ can be represented by the master vector of $\{E_{c,l_c}^m\}$ as

$$\{E_{c,l_c}^s\} = \left[D_{c,l_c}^{ss}\right]^{-1}\left[H_{c,l_c}^{sm}\right]\{E_{c,l_c}^m\} = \left[T_{c,l_c}^{sm}\right]\{E_{c,l_c}^m\} \tag{59}$$

with

$$[D_{c,l_c}^{ss}] = \int_{l_c}\{\mathbf{N}_{c,l_c}^s\}\cdot\{\mathbf{N}_{c,l_c}^s\}^T dl, \quad [H_{c,l_c}^{sm}] = \int_{l_c}\{\mathbf{N}_{c,l_c}^s\}\cdot\{\mathbf{N}_{c,l_c}^m\}^T dl \tag{60}$$

Suppose $[T_{mc}^{sm}]$ consists of all $[T_{c,l_c}^{sm}]$ in the mth subdomain, then we can replace the projection Boolean matrix $[R_{mc}]$ in Eqs. (45)–(48) with $[T_{mc}^{sm}]$.

Similar to SDDM, we can replace Eq. (54) for the non-conformal FETI-DP with:

$$[\tilde{K}_{Sb}]\{u_b\} + [\tilde{K}_{SS}]\{\bar{H}_S\} + [\tilde{K}_{Sc}]\{E_c\} = \{\tilde{f}_S\} \tag{61}$$

where

$$\begin{aligned}
[\tilde{K}_{Sb}] &= [P][T^{SF}]\sum_{m\in\,\text{neighbor}(S)}\Bigg([R_{m,sr}][K_{m,rr}]^{-1}[R_{m,rb}]^T\,[R_{m,Hb}]^T \\
&\qquad \sum_{n\in\,\text{neighbor}(m)}\left([U_{m,mn}\ V_{m,mn}][R_{n,b}]\right)\Bigg) \qquad (62)\\
[\tilde{K}_{SS}] &= [Q] - [P][T^{SF}]\sum_{m\in\,\text{neighbor}(S)}\left([R_{m,sr}][K_{m,rr}]^{-1}[R_{m,ir}]^T[B_{m,iS}]\right) \qquad (63)\\
[\tilde{K}_{Sc}] &= [P][T^{SF}]\sum_{m\in\,\text{neighbor}(S)}\left(-[R_{m,sr}][K_{m,rr}]^{-1}[K_{m,rc}] + I\right)[T_{mc}^{sm}] \qquad (64)
\end{aligned}$$

$$\{\tilde{f}_S\} = \{f_s\} - [P][T^{SF}]\sum_{m\in\,\text{neighbor}(S)}[R_{m,sr}]^T[K_{m,rr}]^{-1}\{f_{m,r}\} \tag{65}$$

By following the same procedure as described in Subsection 2.3, the final matrix equation system only related to unknowns $\{u_b\}$ and $\{\bar{H}_S\}$ can be obtained and solved.

3. NUMERICAL RESULTS AND DISCUSSIONS

The computational complexity of the fast DDMs of FE-BI-MLFMA can be divided into two parts: DDM for FEM and MLFMA for BI. The computational complexity of MLFMA has been well studied and proven to be $N_s \log N_s$ with N_s being the number of surface unknowns [31]. The following will discuss the computational complexity of DDM for FEM. Since FETI-DP DDMs have a more stable convergence speed for the iterative solution to the final interface matrix equation than SDDMs, we will focus on the estimation of computational complexity of FETI-DP DDM.

In FETI-DP DDM, we need to calculate the inverse of the global "corner" matrix $[\tilde{K}_{cc}]$ and $[K_{rr}^i]$ for all subdomains. When the entire FEM domain with N_v unknowns is decomposed into N_a subdomains, the number of unknowns in each subdomain and the number of corner unknowns are $N_r = N_v/N_a$ and $N_c \propto N_a N_r^{1/3} = N_v^{1/3} \times N_a^{2/3}$ respectively. Suppose the computational complexity of sparse direct solvers for the FEM matrix is $O(N^\beta)$ (N is the dimension of the FEM matrix), the computational complexities for performing factorization for all subdomain FEM matrixes and the global corner matrix by using sparse direct solvers are $N_a \times M_{LDL^T}^{D_r} \propto N_a \times (N_r)^\beta = N_a^{1-\beta} N_v^\beta$ and $M_{LDL^T}^{D_c} \propto (N_c)^\beta = N_v^{\beta/3} \times N_a^{2\beta/3}$. If the indexes of β are the same for the inverse of the global matrix $[\tilde{K}_{cc}]$ and $[K_{rr}^i]$ of all subdomains, the computational complexities of these two parts should be equal by setting$N_a = N_v^{2\beta/(5\beta-3)}$. Thus, the computational complexity of the FETI-DP DDM can achieve $O(N_v^{(3\beta^2-\beta)/(5\beta-3)})$. Our following numerical experiments show that the computational complexity of the sparse direct solver of FEM matrix equations is usually less than $O(N_v^2)$, namely $\beta < 2$, for 3D scattering/radiation problems. Hence, the computational complexity of FETI-DP DDM is less than $N_v^{1.43}$. Since the number of surface unknowns N_s usually can be approximated by the number of volume unknowns N_v as $N_s = N_v^{2/3}$, the computational complexity of MLFMA approximately is $N_v^{2/3} \log N_v$. Thus the total computational complexity of FETI-DP DDM of FE-BI-MLFMA should be less than $N_v^{1.43}$.

The above estimation of computational complexity is based on the assumption that the CPU time for the inverse of the global "corner" matrix $[\tilde{K}_{cc}]$ is equal to that for $[K_{rr}^i]$ of all subdomains. It is true for extremely large problems. However, to our often interested problems (i.e., the number of unknowns is less than 1 billion), our numerical experiments show that the CPU time for the inverse of the global "corner" matrix $[\tilde{K}_{cc}]$ is actually a small part of that for $[K_{rr}^i]$ of all subdomains. For these cases, we have a better choice of domain decomposition to obtain better computation efficiency. We fixed the number of unknowns in each subdomain to ten thousands and can achieve nearly linear computational complexity.

Next, we will perform a series of numerical experiments to verify the above analysis of computation efficiency. All the computations are performed on a computer at the Center for Electromagnetic Simulation, Beijing Institute of Technology (BitCEMS). It has 2 Intel X5650 2.66 GHz CPUs with 6 cores for each CPU, 96 GB memory. The GMRES solver is employed with a restart number of 20 and the convergence criterion is set to 0.001. To determine the computational complexity of CPU time and memory, we use the Curve Fitting Tool (cftool) of MATLAB to fit the calculated results. In cftool, the Adjusted R-square (indicator of the fit quality) is set to be larger than 0.995.

First, we need to estimate the computational complexity of direct solver for FEM matrix equations. Among various direct solvers for FEM matrixes, MUMPS is one of the most efficient solvers [32]. Hence, we employ MUMPS to study the computational complexity of direct solvers for the FEM matrix equations numerically. The computational complexity of MUMPS depends on the sparse pattern of the FEM matrix. The sparse pattern of the FEM matrix is determined by the shape of the computational domain. As we know, the shape with almost the same size in the three directions in Cartesian coordinates usually has a larger computational complexity than others with different sizes in the three directions. To be convenient, we take a simple but typical problem, scattering by a dielectric cube with $\varepsilon_r = 4$, as an example. The CPU time and memory for factorizing the FEM matrix of $[K]$ are shown in Fig. 3. We can see the computational complexity for factorizing $[K]$ with MUMPS is about $O(N^{1.85})$ and $O(N^{1.42})$ for CPU time and memory, respectively.

Second, we investigate the computational complexity of computing the inverse of $[\tilde{K}_{cc}]$. We fix the subdomain size as $0.5\lambda \times 0.5\lambda \times 0.5\lambda$ with about 25000 FEM edges. Then we increase the number

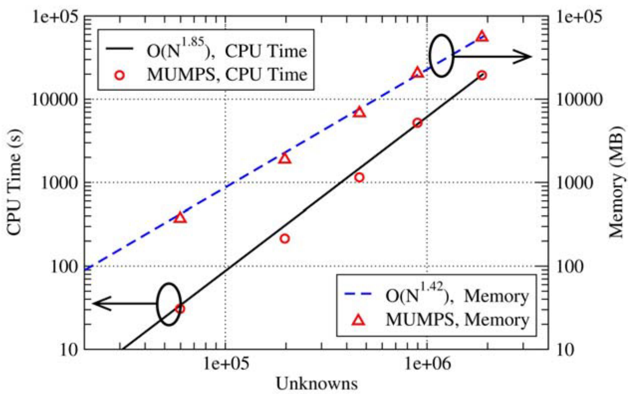

Figure 3. CPU time and memory cost as a function of unknowns for factorizing $[K]$.

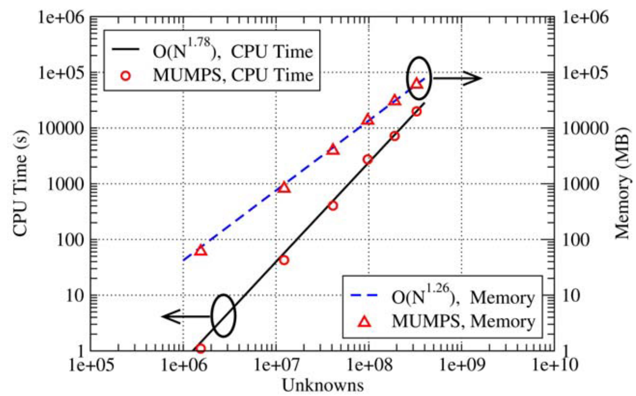

Figure 4. CPU time and memory cost as a function of unknowns for factorizing $[\tilde{K}_{cc}]$.

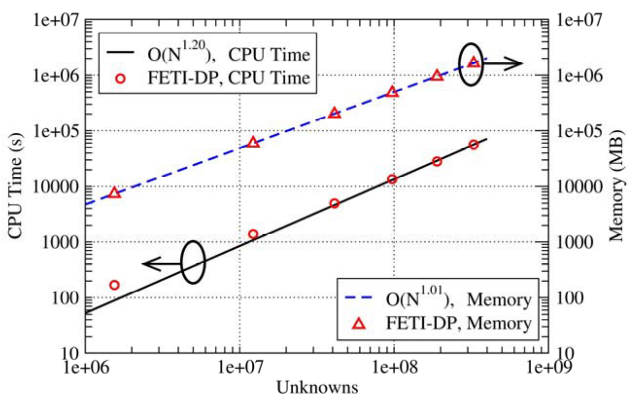

Figure 5. Total CPU time and memory as a function of unknowns for the FETI-DP solution of the FEM equation.

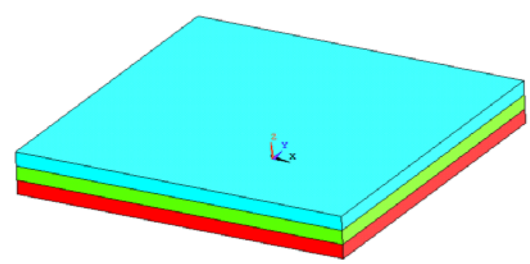

Figure 6. Geometrical configuration of the three layered dielectric brick.

of subdomains from $4 \times 4 \times 4$ to $24 \times 24 \times 24$. Fig. 4 presents the CPU time and memory for computing $[\tilde{K}_{cc}]^{-1}$ as a function of N_v. It can be seen from Fig. 4 that the computational complexity of computing the inverse of $[\tilde{K}_{cc}]$ is about $O(N^{1.78})$ and $O(N^{1.26})$ respectively for the CPU time and memory. Furthermore, we can conclude that the computational complexity of $[\tilde{K}_{cc}]^{-1}$ is smaller than that of $[K]^{-1}$, because the $[\tilde{K}_{cc}]$ is sparser than $[K]$.

Third, we employ the FETI-DP DDM to compute the above examples of the cubes with subdomains from $4\times4\times4$ to $24\times24\times24$. Fig. 5 presents the total CPU time and memory for computing $[\tilde{K}_{cc}]^{-1}$ and all $[K_{rr}^i]^{-1}$ as a function of N_v. We can see from Fig. 5, the computational complexity in FETI-DP is about $O(N^{1.20})$ and $O(N^{1.01})$ respectively for the CPU time and memory. It can be explained as follows. When the subdomain size is fixed, the CPU time and memory for obtaining all $[K_{rr}^i]^{-1}$ increases linearly with the number of total FEM unknowns. In these examples, the CPU time for calculating $[\tilde{K}_{cc}]^{-1}$ is still a small part of that for obtaining all $[K_{rr}^i]^{-1}$. Thus the total CPU and memory of FETI-DP are mainly determined by that for obtaining all $[K_{rr}^i]^{-1}$ and have nearly linear computational complexity.

To further verify the above analysis, an inhomogeneous dielectric brick with three different layers, as shown in Fig. 6, is investigated with FETI-DP DDM of FE-BI-MLFMA. The thickness of each layer is fixed as 0.5λ. The relative permittivity are set to $\varepsilon_1 = 2 - 0.5j$, $\varepsilon_2 = 3 - j$ and $\varepsilon_3 = 4 - 3j$ respectively from the top layer to the bottom layer. Detailed computation information of the three layered inhomogeneous brick with different size is listed in Table 1. The required total CPU time and memory as a function of FEM unknowns are plotted in Fig. 7. We can see from Fig. 7, the CPU time and memory are closer to linear with the number of unknowns than those in Fig. 5. Since the

Table 1. Computation information for the three layered inhomogeneous brick with different sizes.

Brick size (λ)	Domain partion	FEM/BI unknowns	Dual Unknowns	Primal Unknowns	Iteration number
$4 \times 4 \times 1.5$	$8 \times 8 \times 3$	4611885/151200	598560	12285	49
$5 \times 5 \times 1.5$	$10 \times 10 \times 3$	7195845/216000	954600	18645	51
$6 \times 6 \times 1.5$	$12 \times 12 \times 3$	10352205/291600	1393200	26325	53
$8 \times 8 \times 1.5$	$16 \times 16 \times 3$	18382125/475200	2518080	45645	55
$10 \times 10 \times 1.5$	$20 \times 20 \times 3$	28701645/702000	3973200	70245	58
$12 \times 12 \times 1.5$	$24 \times 24 \times 3$	41310765/972000	5758560	100125	60

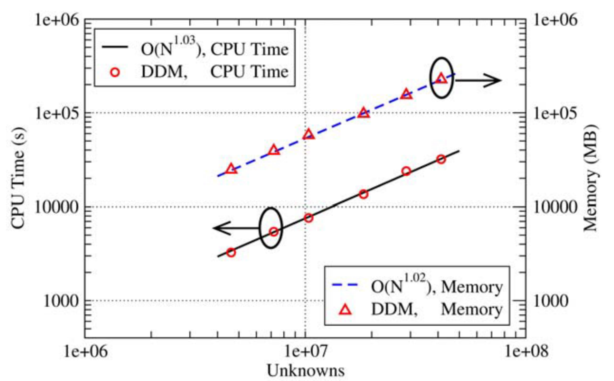

Figure 7. Total CPU time and memory as a function of unknowns for the FETI-DP DDM of FE-BI-MLFMA.

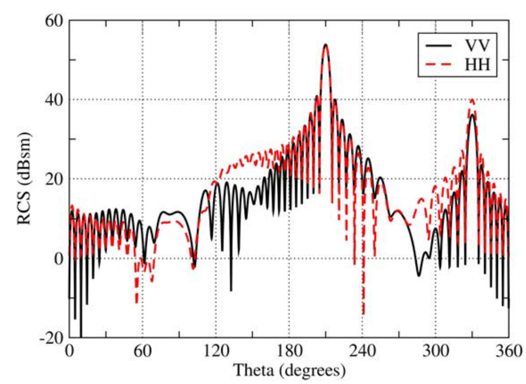

Figure 8. VV and HH-polarized bistatic RCS of the inhomogeneous brick in Fig. 6. The incident angles are set to $\theta = 30°$, $\varphi = 10°$. The observation is in the x-z plane.

size of this example in z-direction is fixed and we just increase the sizes in x- and y-directions, this problem is in fact a 2D extended problem. The number of global corner unknowns is small compared with total number of unknowns. Moreover, the number of iterations for different bricks increases slowly with the total unknowns. Hence the computational complexity is $O(N^{1.03})$ and $O(N^{1.02})$ for CPU time and memory respectively, and an almost linear complexity is achieved. The computed VV and HH polarized bistatic RCSs are shown in Fig. 8.

4. CONCLUSIONS

A unified, consistent, efficient formulation of SDDMs and FETI-DP DDMs of FE-BI-MLFMA is presented for both conformal and non-conformal cases. SDDMs are simple and have easy implementation, whereas FETI-DP DDMs have a more stable and faster convergence. These fast domain decomposition methods can reduce the computational complexity of FE-BI-MLFMA to less than $O(N_v^{(3\beta^2-\beta)/(5\beta-3)})$. For the problems with the number of unknowns less than 1 billion, numerical experiments show that the real computational complexity of FETI-DP DDM of FE-BI-MLFMA can achieve nearly linear computational complexity.

ACKNOWLEDGMENT

This work is partially supported by the National Basic Research Program (973) under Grant No. 61320602 and No. 61327301, the 111 Project of China under the Grant B14010, and the NSFC under Grant 61371002.

REFERENCES

1. Sheng, X. Q., J. M. Jin, J. M. Song, C. C. Lu, and W. C. Chew, "On the formulation of hybrid finite element and boundary integral methods for 3-D scattering," *IEEE Transactions on Antennas and Propagation*, Vol. 46, 303–311, 1998.
2. Sheng, X. Q. and E. K. N. Yung, "Implementation and experiments of a hybrid algorithm of the MLFMA-Enhanced FE-BI method for open-region inhomogeneous electromagnetic problems," *IEEE Transactions on Antennas and Propagation*, Vol. 50, No. 2, 163–167, 2002.
3. Botha, M. M. and J. M. Jin, "On the variational formulation of hybrid finite element-boundary integral techniques for electromagnetic analysis," *IEEE Transactions on Antennas and Propagation*, Vol. 52, No. 11, 3037–3047, 2004.
4. Vouvakis, M. N., S. C. Lee, K. Zhao, and J. F. Lee, "A symmetric FEM-IE formulation with a single-level IE-QR algorithm for solving electromagnetic radiation and scattering problems," *IEEE Transactions on Antennas and Propagation*, Vol. 52, No. 11, 3060–3070, 2004.
5. Liu, J. and J. M. Jin, "A special higher-order finite-element method for scattering by deep cavities," *IEEE Transactions on Antennas and Propagation*, Vol. 48, No. 5, 694–703, 2000.
6. Jin, J. M., J. Liu, Z. Lou, and C. S. T. Liang, "A fully high-order finite-element simulation of scattering by deep cavities," *IEEE Transactions on Antennas and Propagation*, Vol. 51, No. 9, 2420–2429, 2003.
7. Peng, Z. and X. Q. Sheng, "A flexible and efficient higher-order FE-BI-MLFMA for scattering by a large body with deep cavities," *IEEE Transactions on Antennas and Propagation*, Vol. 56, No. 7, 2031–2042, 2008.
8. Yang, M. L. and X.-Q. Sheng, "Parallel high-order FE-BI-MLFMA for scattering by large and deep coated cavities loaded with obstacles," *Journal of Electromagnetic Waves and Applications*, Vol. 23, No. 13, 1813–1823, 2009.
9. Liu, J. and J. M. Jin, "A highly effective preconditioner for solving the finite element-boundary integral matrix equation for 3-D scattering," *IEEE Transactions on Antennas and Propagation*, Vol. 50, 1212–1221, 2002.
10. Hu, F. G. and C. F. Wang, "Preconditioned formulation of FE-BI equations with domain decomposition method for calculation of electromagnetic scattering from cavities," *IEEE Transactions on Antennas and Propagation*, Vol. 57, 2506–2511, 2009.
11. Lee, J., J. Zhang, and C. C. Lu, "Sparse inverse preconditioning of multilevel fast multipole algorithm for hybrid integral equations in electromagnetics," *IEEE Transactions on Antennas and Propagation*, Vol. 52, No. 9, 2277–2287, 2004.
12. Lee, J. F. and D. K. Sun, "p-type multiplicative Schwarz (pMUS) method with vector finite elements for modeling three-dimensional waveguide discontinuities," *IEEE Transactions on Microwave Theory and Techniques*, Vol. 52, No. 3, 864–870, 2004.
13. Yang, M. L. and X. Q. Sheng, "Hybrid h-and p-type multiplicative Schwarz (h-p-MUS) preconditioned algorithm of higher-order FE-BIMLFMA for 3D scattering," *IEEE Transactions on Magnetics*, Vol. 48, 187–190, 2012.
14. Després, B., P. Joly, and J. E. Roberts, "A domain decomposition method for the harmonic Maxwell equations," *Iterative Methods in Linear Algebraic Amsterdam*, 475–484, Elsevier, The Netherlands, 1992.
15. Farhat, C. and F. X. Roux, "A method of finite element tearing and interconnecting and its parallel solution algorithm," *International Journal for Numerical Methods in Engineering*, Vol. 32, 1205–1227, 1991.
16. Wolfe, C. T., U. Navsariwala, and S. D. Gedney, "An efficient implementation of the finite-element time-domain algorithm on parallel computers using finite-element tearing and interconnecting algorithm," *Microwave and Optical Technology Letters*, Vol. 16, No. 4, 1997.
17. Farhat, C., P. Avery, and R. Tezaur, "FETI-DPH: A dual-primal domain decomposition method for acoustic scattering," *Journal of Computational Acoustics*, Vol. 13, 499–524, 2005.

18. Li, Y. J. and J. M. Jin, "A vector dual-primal finite element tearing and interconnecting method for solving 3-D large-scale electromagnetic problems," *IEEE Transactions on Antennas and Propagation*, Vol. 54, 3000–3009, 2006.
19. Li, Y. J. and J. M. Jin, "A new dual-primal domain decomposition approach for finite element simulation of 3-D large-scale electromagnetic problems," *IEEE Transactions on Antennas and Propagation*, Vol. 55, No. 10, 2803–2810, 2007.
20. Yang, M. L. and X. Q. Sheng, "On the finite element tearing and interconnecting method for scattering by large 3D inhomogeneous targets," *International Journal of Antennas and Propagation*, Vol. 2011, 2012, [Online], available: http://www.hindawi.com/journals/ijap/2012/898247/.
21. Zhao, K., V. Rawat, S. C. Lee, and J. F. Lee, "A domain decomposition method with nonconformal meshes for finite periodic and semi-periodic structures," *IEEE Transactions on Antennas and Propagation*, Vol. 55, No. 9, 2559–2570, 2007.
22. Peng, Z. and J. F. Lee, "Non-conformal domain decomposition method with mixed true second order transmission condition for solving large finite antenna arrays," *IEEE Transactions on Antennas and Propagation*, Vol. 59, No. 5, 1638–1651, 2011.
23. Xue, M. F. and J. M. Jin, "Nonconformal FETI-DP methods for large-scale electromagnetic simulation," *IEEE Transactions on Antennas and Propagation*, Vol. 60, No. 9, 4291–4304, 2012.
24. Xue, M. F. and J. M. Jin, "A hybrid conformal/nonconformal domain decomposition method for multi-region electromagnetic modeling," *IEEE Transactions on Antennas and Propagation*, Vol. 62, No. 4, 2009–2021, 2014.
25. Vouvakis, M. N., K. Zhao, S. M. Seo, and J. F. Lee, "A domain decomposition approach for non-conformal couplings between finite and boundary elements for unbounded electromagnetic problems in R^3," *Journal of Computational Physics*, Vol. 225, No. 1, 975–994, 2007.
26. Zhao, K. Z., V. Rawat, S. C. Lee, and J. F. Lee, "Hybrid domain decomposition method and boundary element method for the solution of large array problems," *IEEE Antennas and Propagation Society International Symposium*, 2007.
27. Xue, M. F., Y. J. Li, and J. M. Jin, "Acceleration and accuracy improvement of FEM computation by using FETI-DP and BI hybrid algorithm," *IEEE Antennas and Propagation Society International Symposium*, 2010.
28. Yang, M. L., H. W. Gao, and X. Q. Sheng, "Parallel domain-decomposition-based algorithm of hybrid FE-BI-MLFMA method for 3D scattering by large inhomogeneous objects," *IEEE Transactions on Antennas and Propagation*, Vol. 61, 4675–4683, 2013.
29. Yang, M. L., H. W. Gao, W. Song, and X. Q. Sheng, "An effective domain-decomposition-based preconditioner for the FE-BI-MLFMA method for 3D scattering problems," *IEEE Transactions on Antennas and Propagation*, Vol. 62, No. 4, 2263–2268, 2014.
30. Rao, S. M., D. R. Wilton, and A. W. Glisson, "Electromagnetic scattering by surfaces of arbitrary shape," *IEEE Transactions on Antennas and Propagation*, Vol. 30, 409–418, 1982.
31. Song, J. M., C. C. Lu, and W. C. Chew, "Multilevel fast multipole algorithm for electromagnetic scattering by large complex objects," *IEEE Transactions on Antennas and Propagation*, Vol. 45, No. 10, 1488–1493, 1997.
32. Amestoy, P. R., I. S. Duff, J. Koster, and J.-Y. L'Excellent, "A fully asynchronous multifrontal solver using distributed dynamic scheduling," *SIAM Journal of Matrix Analysis and Applications*, Vol. 23, 15–41, 2001.